Time-reversal-invariant topological superfluids in Bose-Fermi mixtures

Jonatan Melkær Midtgaard,[1] Zhigang Wu,[2] and G. M. Bruun[1]

[1]*Department of Physics and Astronomy, Aarhus University, Ny Munkegade, DK-8000 Aarhus C, Denmark*
[2]*Institute for Advanced Study, Tsinghua University, Beijing 100084, China*

A mixed dimensional system of fermions in two layers immersed in a Bose-Einstein condensate (BEC) is shown to be a promising setup to realize topological superfluids with time-reversal symmetry (TRS). The induced interaction between the fermions mediated by the BEC gives rise to a competition between p-wave pairing within each layer and s-wave pairing between the layers. When the layers are far apart, intralayer pairing dominates and the system forms a topological superfluid either with or without TRS. With decreasing layer separation or increasing BEC coherence length, interlayer pairing sets in. We show that this leads either to a second-order transition breaking TRS where the edge modes gradually become gapped or to a first-order transition to a topologically trivial s-wave superfluid. Our results provide a realistic road map for experimentally realizing a topological superfluid with TRS in a cold atomic system.

I. INTRODUCTION

The search for superfluids and superconductors with non-trivial topological properties has experienced an explosion of activities in recent years. One reason is that these systems can host gapless edge (Majorana) modes with possible applications in quantum computation [1,2]. Excitingly, evidence for topological superconductivity and gapless edge states has been reported in nanowires [3–9]. So far the focus has predominantly been placed on superfluids [10] without time-reversal symmetry (TRS), which belong to the symmetry class D in the tenfold classification scheme of topological insulators and superfluids [11–13]. However, superfluids with TRS, belonging to the class DIII, can also host gapless Majorana mode pairs, which are protected by the Kramers theorem. There are also several proposals to realize such systems in the laboratory, both in condensed-matter systems [14–21] and in cold atomic systems [22–24]. One example of such intriguing systems is the superfluid ^{3}He B phase, the topological properties of which have been studied recently [25,26]. However, one has yet to observe a topological superfluid with TRS in a cold atomic system.

Recently, we showed that a mixed dimensional atomic gas system consisting of a two-dimensional (2D) layer of fermions immersed in a three-dimensional (3D) Bose-Einstein condensate (BEC) constitutes a promising system for realizing a $\mathbb{Z}$ topological superfluid in class D with a high critical temperature [27,28]. Here, we show that an analogous system with two layers of fermions, first studied in Ref. [29], is naturally suited to realize a $\mathbb{Z}_2$ topological superfluid with TRS. Fermions in the layers interact attractively via an induced interaction mediated by the BEC. The relative strengths of the intra- and interlayer induced interaction result in a competition between $p_x \pm ip_y$-wave pairing involving fermions in the same layer, and s-wave pairing involving fermions in different layers. For large distance between the layers, intralayer pairing dominates and one has either a $(p_x + ip_y) \times (p_x - ip_y)$ system with TRS or a $(p_x + ip_y) \times (p_x + ip_y)$ system without TRS. With decreasing layer distance or increasing BEC coherence length, we show that interlayer s-wave pairing occurs in a second-order transition for the $(p_x + ip_y) \times (p_x - ip_y)$ system, which breaks TRS thereby gradually gapping the edge

modes without closing the bulk gap. For short layer distance, the system ends up in a topologically trivial s-wave superfluid, resembling the case of a single layer with two spin components [30]. On the other hand, the transition from the topological $(p_x + ip_y) \times (p_x + ip_y)$ to the trivial s-wave superfluid is of the first order.

II. MODEL

We consider identical (spin polarized) fermions of mass m in two layers located at $z = 0$ and d (see Fig. 1). The fermions are immersed in a 3D gas of bosons with mass m_B and density n_B. The partition function of the system at temperature T is

$$\mathcal{Z} = \int \mathcal{D}(\bar{\psi}_F, \psi_F, \psi_B^*, \psi_B) \, e^{-(S_F + S_B + S_{\text{int}})}, \qquad (1)$$

where $\psi_B(\mathbf{r},\tau)$ and $\psi_F(\mathbf{r},\tau)$ are the bosonic and fermionic fields at point $\mathbf{r}$ and imaginary time τ. The bosons form a weakly interacting BEC that be described by Bogoliubov theory, which yields

$$S_B = \beta \sum_{\mathbf{p}\neq 0, l} \gamma_p^*(-i\omega_l + E_\mathbf{p})\gamma_p \qquad (2)$$

for the bosonic part of the action, where $\beta = 1/T$; $\omega_l = 2l\pi T$ where $l = 0, \pm 1, \pm 2, \ldots$ are the Bose Matsubara frequencies; and γ_p describes the quasiparticle with momentum $\mathbf{p} = (p_x, p_y, p_z)$ and energy $E_\mathbf{p}$. Here we have defined $p \equiv (\mathbf{p}, i\omega_l)$. The Bogoliubov spectrum is $E_\mathbf{p} = \sqrt{\epsilon_\mathbf{p}(\epsilon_\mathbf{q} + 2g_B n_B)}$, where $\epsilon_\mathbf{p} = \mathbf{p}^2/2m_B$ and $g_B = 4\pi a_B/m_B$, where a_B is the boson scattering length. The fermion part of the action is

$$S_F = \beta \sum_{\sigma} \sum_{\mathbf{k}_\perp, j} \bar{a}_{k_\perp\sigma}(-i\omega_j + \xi_{\mathbf{k}_\perp})a_{k_\perp\sigma} \qquad (3)$$

where $a_{k_\perp\sigma}$ are the Grassmann fields for the fermions in layer $\sigma = 1,2$. The effective 2D action for the fermions results from the fact that the vertical trapping potentials are sufficiently tight that the fermions reside only in the lowest trap levels $\phi_0(z)$ and $\phi_0(z - d)$ along the z direction. We have defined $k_\perp \equiv (\mathbf{k}_\perp, i\omega_j)$ with $\mathbf{k}_\perp = (k_x, k_y)$ as the in-plane momentum; $\omega_j = (2j + 1)\pi T$ where $j = 0, \pm 1, \pm 2, \ldots$ are the Fermi Matsubara frequencies; and $\xi_{\mathbf{k}_\perp} = \mathbf{k}_\perp^2/2m - \mu$ where μ is the
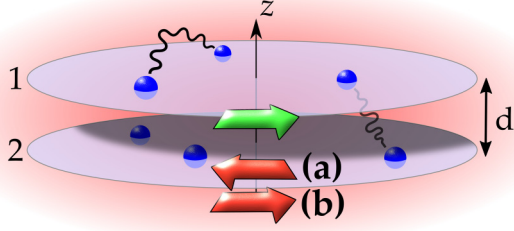
FIG. 1. In the proposed experimental setup, fermions (blue spheres) confined to two layers with distance d interact with the surrounding BEC (red background). This results in induced intralayer and interlayer interactions (illustrated by black wiggly lines). The green and red arrows indicate the edge modes in the two layers, respectively. The intralayer p-wave pairings are either of (a) different chirality, realizing a $\mathbb{Z}_2$ topological superfluid, or of (b) the same chirality, realizing a $\mathbb{Z}$ topological superfluid.

chemical potential of the fermions. We take μ to be the same in each layer which contains an equal number of fermions. Finally, the Bose-Fermi interaction is

$$S_{\text{int}} = g \int d^3r \int_0^\beta d\tau \, \bar{\psi}_F \psi_F \psi_B^* \psi_B, \qquad (4)$$

where g is the boson-fermion interaction strength. Using the Bogoliubov theory to write $\psi_B(\mathbf{r},\tau) = \mathcal{V}^{-1/2} \sum_p (u_{\mathbf{p}} \gamma_p - v_{\mathbf{p}} \gamma_{-p}^*) \exp[i(\mathbf{p} \cdot \mathbf{r} - \omega_l \tau)]$ with $u_{\mathbf{p}}^2, v_{\mathbf{p}}^2 = [(\epsilon_{\mathbf{p}} + g_B n_B)/E_{\mathbf{p}} \pm 1]/2$, and expanding the fermionic fields as $\psi_F(\mathbf{r},\tau) = \sum_{p_\perp,\sigma} a_{p_\perp \sigma} \exp\{i(\mathbf{p} \cdot \mathbf{r}_\perp - \omega_j \tau)\phi_0[z - (\sigma - 1)d]/\sqrt{\mathcal{A}}\}$, we find

$$S_{\text{int}} = \frac{g}{T} \sqrt{\frac{n_B}{\mathcal{V}}} \sum_{\substack{\mathbf{p} \neq 0 \\ l,\sigma}} \sqrt{\frac{\epsilon_{\mathbf{p}}}{E_{\mathbf{p}}}} (\gamma_p + \gamma_p^*) \rho_{p_\perp \sigma} e^{-ip_z d(\sigma-1)} \qquad (5)$$

where $\mathcal{V}$ is the BEC volume, $\mathcal{A}$ is the area of the Fermi layer, $\rho_{p_\perp \sigma} = \sum_{k_\perp} \bar{a}_{k_\perp - p_\perp \sigma} a_{k_\perp \sigma}$, and $p_\perp \equiv (\mathbf{p}_\perp, i\omega_l)$.

Integrating out the quadratic Bose fields in the action in Eq. (1) yields the effective action

$$S_{\text{eff}} = S_F + \frac{\beta}{2\mathcal{A}} \sum_{\substack{p_\perp \\ \sigma, \sigma'}} \rho_{-p_\perp \sigma} V_{\text{ind}}^{\sigma\sigma'}(p_\perp) \rho_{p_\perp \sigma'}, \qquad (6)$$

where the induced interaction between the fermions, mediated by the bosons, is

$$V_{\text{ind}}^{\sigma\sigma'}(p_\perp) = g^2 \int \frac{dp_z}{2\pi} e^{ip_z d(\sigma-\sigma')} \chi_{\text{BEC}}(p). \qquad (7)$$

Here, $\chi_{\text{BEC}}(p) = n_B \mathbf{p}^2 m_B^{-1}/[(i\omega_l)^2 - E_{\mathbf{p}}^2]$ is the density-density correlation function for the BEC and the p_z integration in Eq. (7) is due to the fact that the momentum along the z direction is not conserved in the boson-fermion scattering due to the mixed dimensional setup. We note that the induced interaction in Eq. (7) is obtained with the assumption that the 3D BEC is not affected by the 2D Fermi gases. This is justified in our mixed dimensional setup because the properties of the 3D BEC will only be affected locally in the vicinity of the 2D layers. Since the induced interaction between the fermions is determined by the overall bulk properties of the BEC, we expect that these local effects on the 3D BEC will only lead to

small corrections to the induced interaction given by Eq. (7). For zero frequency, $i\omega_l = 0$, performing the p_z integrals yields

$$V_{\text{ind}}^{\sigma\sigma'}(\mathbf{p}_\perp, 0) = -\frac{2g^2 n_B m_B}{\sqrt{\mathbf{p}_\perp^2 + 2/\xi_B^2}} e^{-d|\sigma-\sigma'|\sqrt{\mathbf{p}_\perp^2 + 2/\xi_B^2}}, \qquad (8)$$

where $\xi_B = (8\pi n_B a_B)^{-1/2}$ is the BEC coherence length. The interlayer ($\sigma \neq \sigma'$) interaction is suppressed compared to the intralayer ($\sigma = \sigma'$) interaction by an exponential factor related to the layer distance d. Fourier transforming Eq. (8) yields a Yukawa interaction $V(\mathbf{r}) = -g^2 n_B m_B \pi^{-1} \exp(-\sqrt{2}r/\xi_B)/r$ in real space with a range determined by ξ_B [28,31–33]. Here $r = |\mathbf{r}|$ is the distance between the particles, which can reside in the same plane or in different planes.

III. GAP EQUATIONS

Since the induced interaction given by Eq. (8) is attractive, fermions with opposite momenta can form Cooper pairs within each layer (intralayer pairing) as well as between different layers (interlayer pairing). The BCS Hamiltonian describing such parings is

$$H_{\text{BCS}} = \frac{1}{2} \sum_{\mathbf{p}} \Psi^\dagger(\mathbf{p}) \mathcal{H}(\mathbf{p}) \Psi(\mathbf{p}), \qquad (9)$$

where $\Psi(\mathbf{p}) = (a_{\mathbf{p}1}, a_{-\mathbf{p}1}^\dagger, a_{\mathbf{p}2}, a_{-\mathbf{p}2}^\dagger)^T$ and

$$\mathcal{H}(\mathbf{p}) = \begin{bmatrix} \xi_{\mathbf{p}} & \Delta_{11}(\mathbf{p}) & 0 & \Delta_{12}(\mathbf{p}) \\ \Delta_{11}^*(\mathbf{p}) & -\xi_{\mathbf{p}} & -\Delta_{12}^*(\mathbf{p}) & 0 \\ 0 & -\Delta_{12}(\mathbf{p}) & \xi_{\mathbf{p}} & \Delta_{22}(\mathbf{p}) \\ \Delta_{12}^*(\mathbf{p}) & 0 & \Delta_{22}^*(\mathbf{p}) & -\xi_{\mathbf{p}} \end{bmatrix}. \qquad (10)$$

Here the $\perp$ subscript is dropped since we are dealing only with 2D momenta of the fermions from now on, and $a_{\mathbf{p}\sigma}$ are the Fermi annihilation operators for layer $\sigma = 1,2$. We neglect retardation effects and use only the zero-frequency component of the induced interaction. Retardation effects are small when the Fermi velocity v_F in the layers is much smaller than the speed of sound in the BEC, while for larger v_F they suppress the magnitude of the pairing without changing the qualitative behavior [27]. The pairing fields are determined self-consistently as

$$\Delta_{\sigma\sigma'}(\mathbf{p}) = -\sum_{\mathbf{k}} V_{\text{ind}}^{\sigma\sigma'}(\mathbf{p} - \mathbf{k}, 0) \langle a_{\mathbf{k}\sigma} a_{-\mathbf{k}\sigma'} \rangle. \qquad (11)$$

We take the interlayer pairing to be s-wave so that $\Delta_{12}(\mathbf{p}) = \Delta_{12}(-\mathbf{p}) = -\Delta_{21}(\mathbf{p})$ and the Fermi antisymmetry dictates that $\Delta_{\sigma\sigma}(\mathbf{p}) = -\Delta_{\sigma\sigma}(-\mathbf{p})$ for the intralayer pairing. Since the system has rotational symmetry with respect to the z axis, we take the intralayer pairing to be of the $p_x \pm ip_y$ form, as this fully gaps the Fermi surface [34], i.e., $\Delta_{\sigma\sigma}(\mathbf{p}) = \Delta_\sigma(|\mathbf{p}|)e^{i\phi_\sigma(\mathbf{p})}$ where $\phi_\sigma(\mathbf{p}) = \phi_{0\sigma} \pm \varphi_{\mathbf{p}}$ with $\varphi_{\mathbf{p}}$ being the azimuthal angle of $\mathbf{p}$. Furthermore, for identical layers we assume that $\Delta_1(|\mathbf{p}|) = \Delta_2(|\mathbf{p}|)$ and we thus have $\Delta_{22}(\mathbf{p}) = \Delta_{11}(\mathbf{p})e^{i[\phi_2(\mathbf{p})-\phi_1(\mathbf{p})]}$. We diagonalize Eq. (9) by introducing new pairing fields $\Delta_\pm(\mathbf{p}) = \Delta_{11}(\mathbf{p}) \pm \Delta_{12}(\mathbf{p})e^{-i[\phi_2(\mathbf{p})-\phi_1(\mathbf{p})-\pi]/2}$. Equation (11) then yields

a set of gap equations in a symmetrical form as

$$\Delta_\nu(\mathbf{p}) = -\sum_{\nu',\mathbf{k}} V_{\nu\nu'}(\mathbf{p} - \mathbf{k}) \frac{\Delta_{\nu'}(\mathbf{k})}{2E_{\mathbf{k},\nu'}} \tanh\left(\frac{E_{\mathbf{k},\nu'}}{2T}\right). \quad (12)$$

Here $\nu = \pm$, $E_{\mathbf{p},\pm} = \sqrt{\xi_\mathbf{p}^2 + |\Delta_\pm(\mathbf{p})|^2}$, and

$$V_{\nu\nu'}(\mathbf{p} - \mathbf{k}) \equiv \frac{1}{2}\big[V_{\mathrm{ind}}^{11}(\mathbf{p} - \mathbf{k}) + \mathrm{sgn}(\nu,\nu')e^{-i[\phi_2(\mathbf{p})-\phi_1(\mathbf{p})]/2}$$
$$\times V_{\mathrm{ind}}^{12}(\mathbf{p} - \mathbf{k})e^{i[\phi_2(\mathbf{k})-\phi_1(\mathbf{k})]/2}\big], \quad (13)$$

where $\mathrm{sgn}(\nu,\nu) = 1$ and $\mathrm{sgn}(\nu,-\nu) = -1$. Finally, the number equation is $N = \sum_{\nu,\mathbf{p}}[1 - \xi_\mathbf{p}\tanh(E_{\mathbf{p},\nu}/2T)/E_{\mathbf{p},\nu}]/2$ and the BCS ground-state energy is

$$E_{\mathrm{BCS}} - \mu N = \frac{1}{2}\sum_{\nu,\mathbf{p}}[\xi_\mathbf{p} - E_{\mathbf{p},\nu} + |\Delta_{\mathbf{p},\nu}|^2/2E_{\mathbf{p},\nu}]. \quad (14)$$

We note that when the s- and p-wave order parameters coexist their relative phase is important. It cannot be gauged away contrary to the case of a single order parameter. The relative phase therefore has physical consequences, and we shall see that it determines whether the system has a time-reversal symmetry or not.

IV. SYMMETRIES AND TOPOLOGICAL PROPERTIES

The topological properties of the bilayer system are determined by its symmetries and 2D dimensionality [11–13]. Consider first the limit where the two layers are uncoupled, which corresponds to the layer distance being much larger than the range of the induced interaction given by the BEC coherence length, i.e., $d \gg \xi_\mathrm{B}$. There is then only particle-hole symmetry for each layer, and they each form a topological $p_x \pm ip_y$ superfluid in symmetry class D, which supports chiral edge states. Consider now the case when the two layers are brought closer to each other so that they interact. The topological properties and the fate of the edge states then depend on whether the Cooper pairs in the two layers have opposite or the same angular momentum, corresponding to $(p_x + ip_y) \times (p_x - ip_y)$ or $(p_x + ip_y) \times (p_x + ip_y)$ pairing, respectively.

For $(p_x + ip_y) \times (p_x - ip_y)$ pairing illustrated in Fig. 1(a), which we refer to as the $(+,-)$ case, the system possesses in addition to particle-hole symmetry the time-reversal symmetry

$$\mathcal{T}(a_{\mathbf{p}1},a_{\mathbf{p}2})\mathcal{T}^{-1} = (a_{-\mathbf{p}2}, -a_{-\mathbf{p}1}), \quad (15)$$

which swaps particles in the two layers. Note that this antiunitary symmetry operation is different from the usual time-reversal symmetry operation, which flips the spin of the particles. Here, the layer index plays the role of a pseudospin. Since $\mathcal{T}^2 = -1$, the bilayer system is then in symmetry class DIII, and its ground state is a $\mathbb{Z}_2$ topological superfluid, which supports helical edge modes in analogy with the quantum

spin Hall state [35–37]. The counterpropagating edge modes in the two layers are related by TRS and protected by the Kramers theorem. However, when the layers are sufficiently close together, the s-wave interlayer pairing ($\Delta_{12}(\mathbf{p}) \neq 0$) will dominate, and the system forms a topologically trivial s-wave superfluid. Thus, the edge states must become gapped at some critical interlayer distance. Without solving the gap equation, one can envision two ways this can happen: either the interlayer pairing explicitly breaks TRS thereby gapping the edge modes as soon as $\Delta_{12}(\mathbf{p}) \neq 0$, or the interlayer pairing respects TRS and the edge states become gapped only when the bulk energy gap is closed. By analyzing the properties of the interlayer gap under time reversal, we find that these two scenarios correspond to $\Delta_{12}(\mathbf{p})$ being imaginary and real, respectively. Our numerical results (see later) show that $\Delta_{12}(\mathbf{p})$ is in fact imaginary and the first scenario describes the physical transition.

For $(p_x + ip_y) \times (p_x + ip_y)$ pairing illustrated in Fig. 1(b), which we refer to as the $(+,+)$ case, the system only has the particle-hole symmetry and is a $\mathbb{Z}$ topological superfluid in class D, which supports chiral edge modes propagating in the same direction in the two layers. When the layer distance is decreased, the possible onset of interlayer pairing coexisting with the intralayer pairing will not gap these edge modes as long as the bulk gap remains nonzero, since this pairing does not break any symmetry. However, we shall see later that such a coexisting scenario does not occur for the $(+,+)$ case. Similar to the $(+,-)$ case, the system ends up in the topologically trivial interlayer s-wave superfluid for small interlayer distances. We shall demonstrate below that this happens via a first-order phase transition.

The topological $\mathbb{Z}$ and $\mathbb{Z}_2$ invariants of class D and DIII, respectively, can be calculated from the two energy bands $E_{\mathbf{p},+}$ and $E_{\mathbf{p},-}$ of the bilayer system [38]. If the two layers are uncoupled, these bands are degenerate and the invariant for class D is simply given by the sum $C = C_1 + C_2$ of the Chern numbers C_σ of each layer, whereas it is given by the difference $\nu = C_1 - C_2 \pmod 2$ for class DIII. This is consistent with the fact that the $(+,-)$ state has $C_1 = -1, C_2 = 1$ and is therefore topological in class DIII, whereas it is trivial in class D. Therefore, if the TR symmetry is broken for the $(+,-)$ state by an imaginary $\Delta_{12}(\mathbf{p})$ that mixes the two bands, the system is in class D and it is no longer topological.

V. EDGE STATES

In this section, we show explicitly how the edge states of the $(+,-)$ system become gapped with the onset of interlayer s-wave pairing $\Delta_{12}(\mathbf{p})$ which is imaginary. We consider the following low-energy Hamiltonian in real space:

$$H = \int d^2\mathbf{r}\,\Psi^\dagger(\mathbf{r})\mathcal{H}(\mathbf{r})\Psi(\mathbf{r})$$

where $\Psi(\mathbf{r}) = (\psi_1,\psi_1^\dagger,\psi_2,\psi_2^\dagger)^T$ and

$$\mathcal{H}(\mathbf{r}) = \begin{pmatrix} -\mu(\mathbf{r}) & \Delta_{11}e^{-i\phi_0}(-\partial_x + i\partial_y) & 0 & \Delta_{12} \\ \Delta_{11}e^{i\phi_0}(\partial_x + i\partial_y) & \mu(\mathbf{r}) & -\Delta_{12}^* & 0 \\ 0 & -\Delta_{12} & -\mu(\mathbf{r}) & \Delta_{11}e^{i\phi_0}(-\partial_x - i\partial_y) \\ \Delta_{12}^* & 0 & \Delta_{11}e^{-i\phi_0}(\partial_x - i\partial_y) & \mu(\mathbf{r}) \end{pmatrix}.$$

Assuming that we can apply a local-density approximation, we take $\mu(\mathbf{r}) = \mu(r)$ to be positive within the radius R, and negative outside. Solutions to the eigenvalue equation $\mathcal{H}(\mathbf{r})\chi(\mathbf{r}) = E\chi(\mathbf{r})$ with definite angular momentum can then be found, and we use the following ansatz in the usual polar coordinates:

$$\chi(\mathbf{r}) = \kappa e^{in\theta} \begin{pmatrix} e^{-i\phi/2}[A(r) + iB(r)] \\ e^{i\phi/2}[A(r) - iB(r)] \\ e^{i\phi/2}[C(r) + iD(r)] \\ e^{-i\phi/2}[-C(r) + iD(r)] \end{pmatrix}$$

where κ is a normalization constant. The real functions A, B, C, D satisfy a set of four coupled equations, and for a large system with tightly confined edge modes we can find solutions with the energy $\pm E = \pm\sqrt{(\Delta_{11}n/R)^2 + |\Delta_{12}|^2}$. Here, n is a half integer related to the angular momentum of the edge state. These solutions require Δ_{12} to be real. If it is imaginary, it is possible to show that the edge modes do not acquire a gap. When finding the specific solutions for the edge states, care should be taken to choose the solution that is normalizable and confined to the edge. As an example, consider the physical, positive branch of energies, $+E$. A possible solution is given by $A(r) = D(r) = 0$ and

$$B(r) = \exp\left\{\frac{1}{\Delta_{11}}\int_0^r \mu(r')dr'\right\}$$

$$C(r) = \alpha B(r)$$

with

$$\alpha = \frac{\Delta_{11}n}{|\Delta_{12}|R} - \sqrt{\left(\frac{\Delta_{11}n}{|\Delta_{12}|R}\right)^2 + 1}.$$

We see that the edge states lowest in energy are localized on both layers when the two gap parameters coexist. The states higher in energy approach the solutions for uncoupled layers, which are only localized on a single layer.

VI. NUMERICAL SOLUTION OF THE GAP EQUATION

We now numerically solve the gap equations (12) along with the number equation at $T = 0$. The $(+, -)$ case corresponds to $\phi_2(\mathbf{p}) - \phi_1(\mathbf{p}) = \pi - 2\varphi_{\mathbf{p}}$, while the $(+, +)$ case corresponds to $\phi_2(\mathbf{p}) - \phi_1(\mathbf{p}) = \pi$.

A. $(+, -)$ system

In Fig. 2(a), we plot the magnitude of the pairing fields at the Fermi surface as a function of the layer distance d for the $(+, -)$ system. Here $k_F = \sqrt{4\pi n_F}$ is the Fermi momentum with n_F the density of fermions in each layer. We have chosen a relatively weak Bose-Fermi coupling strength $g = 2\pi a/\sqrt{m_r m_B}$ with $k_F a = 0.1$, where a is the 2D-3D mixed dimensional scattering length [39]. The gas parameter of the BEC is $(n_B a_B^3)^{1/3} = 0.01$ and the ratio of the Fermi and Bose interparticle distances is $n_F^{1/2}/n_B^{1/3} = 0.2$. The energy of the system is plotted in Fig. 2(b).

For layer distances $d \gtrsim 0.754\xi_B$, there is no interlayer pairing and the two layers are uncoupled, each realizing a $p_x \pm ip_y$ topological superfluid. The corresponding edge
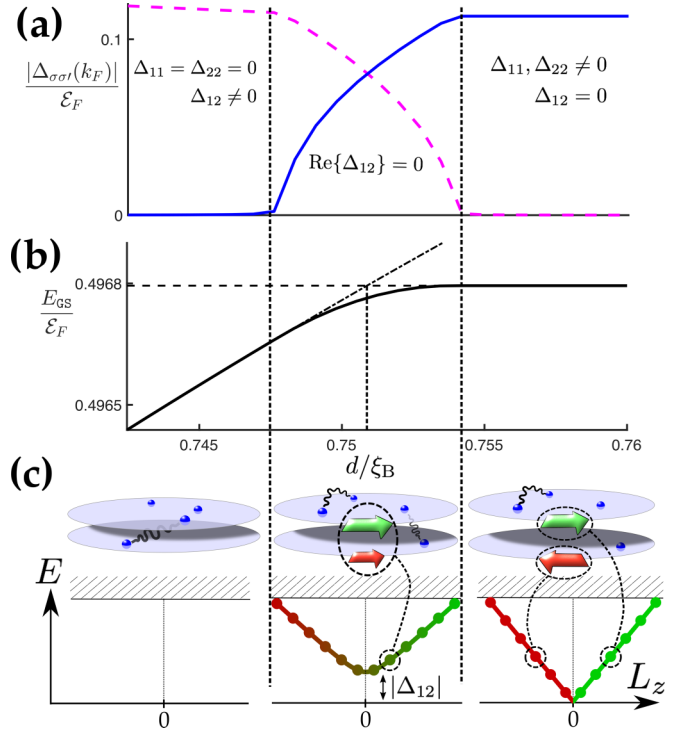

FIG. 2. (a) The magnitude of the interlayer s-wave pairing (dashed line) and intralayer p-wave pairing (solid line) as a function of the layer distance for the $(+, -)$ system. (b) The corresponding ground-state energy per particle (solid line). The dashed lines indicate the energy of states with only inter- or intralayer pairing. The dashed vertical line at $d \simeq 0.751\xi_B$ indicates where the two solutions have the same energy. (c) The edge modes of the $(+, -)$ system and their spectrum. For $d \gtrsim 0.754\xi_B$ (right column) the counter clockwise and clockwise edge modes are localized in the upper and lower layer, respectively. For $0.747\xi_B \lesssim d \lesssim 0.754\xi_B$ (middle column), the low-lying edge modes are localized in both layers and they acquire a gap. For $d \lesssim 0.747\xi_B$ (left column), there are no edge modes.

states, illustrated in Fig. 2(c), propagate in opposite directions in the two layers and are related by the TRS operator $\mathcal{T}$. We have chosen a circular boundary with radius R to illustrate the typical geometry formed by the harmonic trap in an atomic gas experiment. As the layer distance decreases, interlayer pairing sets in for $d \lesssim 0.754\xi_B$ via a second-order transition and it coexists with the intralayer pairing. We find numerically that the interlayer pairing $\Delta_{12}(\mathbf{k})$ is purely imaginary and it therefore breaks TRS. The edge modes in the two layers mix and become gapped as illustrated in Fig. 2(c). More precisely, the dispersion of the edge modes is $E = \sqrt{(\Delta_{11}n/R)^2 + |\Delta_{12}|^2}$, where $|\Delta_{12}| \simeq |\Delta_{12}(0)|$ and $\Delta_{11}(\mathbf{p}) \simeq \Delta_{11}(p_x + ip_y)$ give the magnitude of the inter- and intralayer pairing at low momenta, as seen above. The low-energy edge states with small n are hybridized between the two layers; for larger n, the edge states become increasingly localized in a single layer, approaching those for the uncoupled layers. Finally, for layer distances $d \lesssim 0.747\xi_B$ the intralayer pairing is completely suppressed by the interlayer pairing and the system is a topologically trivial s-wave superfluid with no edge modes. We have not been
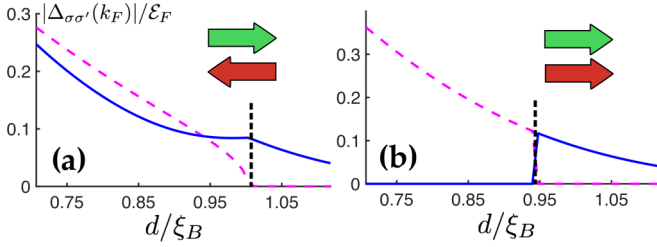
FIG. 3. The intra- (solid line) and interlayer (dashed line) pairing as a function of the BEC coherence length for the (a) $(+,-)$ and (b) $(+,+)$ system.

able to find a numerical solution with a real interlayer pairing coexisting with intralayer pairing, which would preserve TRS and support the gapless edge modes. While the coexistence region shown here is quite narrow, the width can be tuned by altering the parameters (see below).

B. $(+,+)$ system

For the $(+,+)$ system, our numerical results show that the transition between the topological and trivial phase is first order. The transition occurs at the critical layer distance $d \simeq 0.751\xi_B$ when the phases with only one type of pairing have the same energy, as indicated by the vertical line in Fig. 2(b). We do not find numerical solutions with both types of pairing coexisting. Instead, the intralayer pairing and the associated gapless edge modes disappear and the interlayer pairing appears abruptly.

VII. VARYING THE COHERENCE LENGTH

Experimentally, it might be easier to change the BEC coherence length, which determines the range of the induced interaction, by varying a_B using a Feshbach resonance, instead of changing the layer distance. To examine this case, we plot in Fig. 3 the magnitudes of the intra- and interlayer pairings as a function of ξ_B with $k_F a = 0.12$, $k_F d = 1.0$, and $n_F^{1/2}/n_B^{1/3} = 0.2$. The coherence length is varied by changing a_B keeping n_B fixed. For a small ξ_B, the two layers are uncoupled forming the $(+,-)$ or the $(+,+)$ topological superfluid. The $(+,-)$ system undergoes a second-order phase transition to a state where intra- and interlayer pairings coexist for $\xi_B \gtrsim 1d$. Note that contrary to decreasing the distance d the system does not end up in a pure s-wave state for large ξ_B. The reason is that for a large interaction range the suppression of the p-wave channel compared to the s-wave channel is small, and intra-

and interlayer pairings therefore coexist. The $(+,+)$ system on the other hand again undergoes a first-order transition between the topological and the trivial phases at $\xi_B \sim 1.05d$.

VIII. DISCUSSION

All the ingredients in the proposed setup have been realized experimentally. Bose-Fermi mixtures as well as species selective optical potentials to produce mixed dimensional systems have been reported [40–42]. It was moreover shown in Ref. [27] that the Berezinskii-Kosterlitz-Thouless critical temperature for the $p_x \pm ip_y$ superfluid in the present Bose-Fermi setup can be as high as $T_{\mathrm{BKT}} = \mathcal{E}_F/16$, which is within experimental reach [43]. We expect the critical temperature of the phase with s-wave pairing to be even higher. The edge modes can be observed for instance by direct imaging or by the response to an external drive in analogy with topological insulators [44–46].

An intriguing question concerns the robustness of the edge modes beyond mean-field BCS theory. To investigate this, one could analyze the coupling between the edge modes forming a Luttinger liquid [47,48], which is an interesting future project.

IX. CONCLUSION

We demonstrated that a mixed dimensional system consisting of two layers of fermions in a BEC is a powerful setup to realize topological superfluids with TRS. The induced interaction between the fermions mediated by the BEC leads to a competition between p-wave pairing within each layer and s-wave pairing between the layers. For large layer separation or short BEC coherence length, intralayer pairing dominates and the system forms a topological superfluid either with or without TRS. In the case of TRS, the system goes from a $\mathbb{Z}_2$ topological superfluid to a topologically trivial superfluid via a second-order transition where s-wave pairing gradually gaps the edge modes. When there is no TRS, the transition from a $\mathbb{Z}$ topological superfluid to a topologically trivial superfluid is first order. These results show how cold atomic gases offer a realistic path to realizing topological superfluids with TRS.

ACKNOWLEDGMENTS

[1] J. Alicea, Rep. Prog. Phys. **75**, 076501 (2012).

[2] C. Nayak, S. H. Simon, A. Stern, M. Freedman, and S. Das Sarma, Rev. Mod. Phys. **80**, 1083 (2008).

[3] V. Mourik, K. Zuo, S. M. Frolov, S. R. Plissard, E. P. A. M. Bakkers, and L. P. Kouwenhoven, Science **336**, 1003 (2012).

[4] M. T. Deng, C. L. Yu, G. Y. Huang, M. Larsson, P. Caroff, and H. Q. Xu, Nano Lett. **12**, 6414 (2012).

[5] A. Das, Y. Ronen, Y. Most, Y. Oreg, M. Heiblum, and H. Shtrikman, Nat. Phys. **8**, 887 (2012).

[6] L. P. Rokhinson, X. Liu, and J. K. Furdyna, Nat. Phys. **8**, 795 (2012).

[7] A. D. K. Finck, D. J. Van Harlingen, P. K. Mohseni, K. Jung, and X. Li, Phys. Rev. Lett. **110**, 126406 (2013).

[8] S. Nadj-Perge, I. K. Drozdov, J. Li, H. Chen, S. Jeon, J. Seo, A. H. MacDonald, B. A. Bernevig, and A. Yazdani, Science **346**, 602 (2014).

[9] S. M. Albrecht, A. P. Higginbotham, M. Madsen, F. Kuemmeth, T. S. Jespersen, J. Nygård, P. Krogstrup, and C. M. Marcus, Nature (London) **531**, 206 (2016).

[10] We shall from now on refer to superfluids only. It is implicitly understood that this also refers to superconductors.

[11] A. P. Schnyder, S. Ryu, A. Furusaki, and A. W. W. Ludwig, Phys. Rev. B **78**, 195125 (2008).

[12] A. Kitaev, AIP Conf. Proc. **1134**, 22 (2009).

[13] A. Altland and M. R. Zirnbauer, Phys. Rev. B **55**, 1142 (1997).

[14] C. L. M. Wong and K. T. Law, Phys. Rev. B **86**, 184516 (2012).

[15] S. Deng, L. Viola, and G. Ortiz, Phys. Rev. Lett. **108**, 036803 (2012).

[16] F. Zhang, C. L. Kane, and E. J. Mele, Phys. Rev. Lett. **111**, 056402 (2013).

[17] S. Nakosai, J. C. Budich, Y. Tanaka, B. Trauzettel, and N. Nagaosa, Phys. Rev. Lett. **110**, 117002 (2013).

[18] A. Keselman, L. Fu, A. Stern, and E. Berg, Phys. Rev. Lett. **111**, 116402 (2013).

[19] E. Gaidamauskas, J. Paaske, and K. Flensberg, Phys. Rev. Lett. **112**, 126402 (2014).

[20] J. Klinovaja, A. Yacoby, and D. Loss, Phys. Rev. B **90**, 155447 (2014).

[21] C. Schrade, A. A. Zyuzin, J. Klinovaja, and D. Loss, Phys. Rev. Lett. **115**, 237001 (2015).

[22] Z. Yan, X. Yang, and S. Wan, Eur. Phys. J. B **86**, 347 (2013).

[23] X. Yang, B. Huang, and H.-Q. Lin, J. Phys. B **46**, 205302 (2013).

[24] B. Huang, P. H. Chui, J. Liu, C. Zhang, and M. Gong, arXiv:1511.01713.

[25] G. E. Volovik, JETP Lett. **90**, 587 (2009).

[26] Y. Makhlin, M. Silaev, and G. E. Volovik, Phys. Rev. B **89**, 174502 (2014).

[27] Z. Wu and G. M. Bruun, Phys. Rev. Lett. **117**, 245302 (2016).

[28] J. M. Midtgaard, Z. Wu, and G. M. Bruun, Phys. Rev. A **94**, 063631 (2016).

[29] Y. Nishida, Phys. Rev. A **82**, 011605 (2010).

[30] T. Anzai and Y. Nishida, Phys. Rev. A **95**, 051603 (2017).

[31] M. J. Bijlsma, B. A. Heringa, and H. T. C. Stoof, Phys. Rev. A **61**, 053601 (2000).

[32] L. Viverit, C. J. Pethick, and H. Smith, Phys. Rev. A **61**, 053605 (2000).

[33] D. Suchet, Z. Wu, F. Chevy, and G. M. Bruun, Phys. Rev. A **95**, 043643 (2017).

[34] P. W. Anderson and P. Morel, Phys. Rev. **123**, 1911 (1961).

[35] C. L. Kane and E. J. Mele, Phys. Rev. Lett. **95**, 146802 (2005).

[36] C. L. Kane and E. J. Mele, Phys. Rev. Lett. **95**, 226801 (2005).

[37] X.-L. Qi, T. L. Hughes, S. Raghu, and S.-C. Zhang, Phys. Rev. Lett. **102**, 187001 (2009).

[38] J. de Lisle, S. De, E. Alba, A. Bullivant, J. J. Garcia-Ripoll, V. Lahtinen, and J. K. Pachos, New J. Phys. **16**, 083022 (2014).

[39] Y. Nishida and S. Tan, Phys. Rev. Lett. **101**, 170401 (2008).

[40] G. Lamporesi, J. Catani, G. Barontini, Y. Nishida, M. Inguscio, and F. Minardi, Phys. Rev. Lett. **104**, 153202 (2010).

[41] D. C. McKay, C. Meldgin, D. Chen, and B. DeMarco, Phys. Rev. Lett. **111**, 063002 (2013).

[42] G. Jotzu, M. Messer, F. Görg, D. Greif, R. Desbuquois, and T. Esslinger, Phys. Rev. Lett. **115**, 073002 (2015).

[43] R. Onofrio, Phys. Usp. **59**, 1129 (2017).

[44] N. Goldman, J. Dalibard, A. Dauphin, F. Gerbier, M. Lewenstein, P. Zoller, and I. B. Spielman, Proc. Natl. Acad. Sci. USA **110**, 6736 (2013).

[45] D. T. Tran, A. Dauphin, A. G. Grushin, P. Zoller, and N. Goldman, Sci. Adv. **3**, e1701207 (2017).

[46] N. Goldman, G. Jotzu, M. Messer, F. Görg, R. Desbuquois, and T. Esslinger, Phys. Rev. A **94**, 043611 (2016).

[47] C. Xu and J. E. Moore, Phys. Rev. B **73**, 045322 (2006).

[48] Y. Tanaka and N. Nagaosa, Phys. Rev. Lett. **103**, 166403 (2009).